Hindawi
Mathematical Problems in Engineering
Volume 2018, Article ID 3528092, 13 pages
https://doi.org/10.1155/2018/3528092

Research Article

Adaptive Finite-Time Control for Formation Tracking of Multiple Nonholonomic Unmanned Aerial Vehicles with Quantized Input Signals

Jinglin Hu, Xiuxia Sun, and Lei He

Air Force Engineering University, Xi'an 710038, China

Correspondence should be addressed to Jinglin Hu; hujinglineee@163.com

Received 7 March 2018; Accepted 16 May 2018; Published 11 June 2018

Academic Editor: Yakov Strelniker

Signal quantization can reduce communication burden in multiple unmanned aerial vehicle (multi-UAV) system, whereas it brings control challenge to formation tracking of multi-UAV system. This study presents an adaptive finite-time control scheme for formation tracking of multi-UAV system with input quantization. The UAV model contains nonholonomic kinematic model and autopilot model with uncertainties. The nonholonomic states of the UAVs are transformed by a transverse function method. For input quantization, hysteretic quantizers are used to reduce the system chattering and new decomposition is introduced to analyze the quantized signals. Besides, a novel transformation of the control signals is designed to eliminate the quantization effect. Based on the backstepping technique and finite-time Lyapunov stability theory, the adaptive finite-time controller is established for formation tracking of the multi-UAV system. Stability analysis proves that the tracking error can converge to an adjustable small neighborhood of the origin within finite time and all the signals in closed-loop system are semiglobally finite-time bounded. Simulation experiment illustrates that the system can track the reference trajectory and maintain the desired formation shape.

1. Introduction

Recent years have seen an increasing amount of concerns in theoretical researches and practical applications of multiagent systems [1]. As a kind of typical multiagent systems, multi-UAV system can be used in more applications if they are equipped with formation tracking ability [2]. Formation tracking is achieved when all the UAVs in a system can track the reference trajectory and maintain a desired formation shape [3]. Formation tracking brings control challenges to multi-UAV systems, and it has been studied in many early researches [4–6]. Notably, these early efforts mainly assume that communication capacity among the UAVs is accurate and limitless. Indeed, formation communication is constrained because of limited channel bandwidth in multi-UAV systems. To reduce communication burden, control or measurement signals are always processed before being transmitted through communication networks by quantizers. The quantizer is regarded as a discontinuous map from continuous regions to a finite discrete set [7]. However, quantization introduces strong nonlinear characteristics, which may cause the systems to have worse transient performance or even instability [8, 9].

It is important to take quantization into consideration in formation tracking control of multi-UAV systems. In quantized control systems, signals are always processed by various kinds of quantizers. The most commonly used quantizers are uniform quantizer and logarithmic quantizer. Uniform quantizer was used in a stabilization control scheme of linear systems to process input signals [10]. However, uniform quantizer can only lead to practical stability of control systems because of fixed quantization levels [11]. To overcome the weakness of uniform quantizer, logarithmic quantizer was introduced by increasing quantization levels near the origin. In [12], it was proved that logarithmic quantizer is the coarsest quantizer to achieve quadratic stabilization of linear systems. To avoid the system chattering caused by logarithmic quantizer, hysteretic quantizer was used in a stabilization control scheme by taking derivative information of signals into quantizer [13]. Based on backstepping technique, an adaptive

control scheme is proposed for stabilization of nonlinear system with input signals being processed by hysteretic quantizer [14]. However, the nonlinearity introduced by hysteretic quantizer even makes it difficult for the existing stabilization schemes to be extended to tracking control problems, let alone to achieve trajectory tracking with guaranteed transient performance, such as finite-time convergence.

On the other hand, many quantized control strategies have been done for multiagent systems with linear agent dynamics. In [15], by using uniform quantized communication, the authors proposed a gossip consensus algorithm for formation tracking of multiagent systems with linear discrete-time agent dynamics. With both uniform and logarithmic quantized information considered, an adaptive coordinated formation tracking strategy was proposed for continuous-time first-order integrator multiagent systems [16]. To improve model precision, some researchers describe UAV dynamics as nonlinear strict feedback models with uncertainties, such as unknown parameters or disturbances. With logarithmically quantized state measurements, an impulsive control strategy was proposed for formation tracking problem of multiagent systems with nonlinear dynamics [17]. Under leader-following structure, a formation tracking algorithm was proposed for second-order multiagent systems with uncertain nonlinear dynamics [18]. However, most practical applications of formation tracking control involve the agents that are nonholonomically constrained or underactuated. The multiagent systems with nonholonomic constraints cannot be controlled by simply using some control strategies like strict feedback systems. The most commonly considered nonholonomic agents are underactuated surface vessels (USVs) and wheeled mobile robots. In [19], the authors proposed an output feedback control approach for reference tracking of USVs. A cooperative quantized control scheme was proposed for a group of wheeled mobile robots with nonholonomic constraints [20]. These nonholonomic models of USVs or mobile robots cannot be applied to describe the kinematic and dynamic models of UAVs. It should be mentioned that there are few investigations about quantized control for formation tracking of multiple UAVs with nonholonomic constraints and uncertainties.

The control approaches in the aforementioned papers can only guarantee that the tracking errors converge to the equilibrium with time going to infinity. On the basis of system stability, controller designs are always required to possess good transient performance. Due to some mission requirements, finite-time control schemes are investigated for formation tracking of multiple agents recently. In [21], finite-time stabilization problem was investigated for a class of high order nonholonomic systems. A homogeneous feedback control strategy was proposed for the finite-time convergence of quadrotor trajectory tracking [22]. Despite the results presented in [21, 22], the finite-time controllers are still limited to agents with completely known models or uncertainties which are bounded by known constants or continuous functions. Notably, the adaptive finite-time control schemes remain open for multiple nonholonomic UAVs with quantized input and uncertainties to the best of our knowledge.

Motivated by the above discussion, we investigates the formation tracking problem of the multi-UAV systems with quantized input signals via an adaptive backstepping based finite-time control scheme. In addition, the UAVs contain nonholonomic kinematic model and autopilot model with uncertainties. These uncertainties mainly indicate unknown parameters and time-varying disturbances with unknown bounds. The main contributions are listed as follows.

(i) The conventional controller for strict feedback systems cannot be applied to tracking control of the multiple nonholonomic UAVs. The UAV states with nonholonomic constraints are transformed by a transverse function method. The unknown parameters and disturbances in the models are estimated by several tuning functions in the control design.

(ii) To avoid system chattering, input signals are processed by hysteretic quantizer. Many restrictions in [13, 14] are released through using new decomposition to the quantized signals. In contrast to the control signals of traditional backstepping controller, a novel transformation is introduced for the control signals to eliminate the quantization effect. In addition, a coarser quantization can be used in controller, which can reduce the communication burden more effectively.

(iii) The systems are always completely known or have uncertainties with known bounds in the existing finite-time control schemes. Compared with the existing finite-time controllers, the system in our proposed control scheme has unknown parameters and time-varying disturbances, which have unknown bounds. We design the novel tuning functions to estimate the uncertainties for satisfying the system stability and the finite-time convergence of formation tracking. An adaptive finite-time control scheme is established by using finite-time Lyapunov stability theory. With the proposed finite-time controller, the trajectory tracking errors can be steered to within an adjustable small neighborhood of the origin in finite time. All the signals in the closed-loop system are semiglobally finite-time bounded.

The remainder of this paper is organized as follows: Section 2 introduces the control problem and some preliminaries. An adaptive finite-time control scheme is proposed for formation tracking control in Section 3. Section 4 analyzes the stability of the control scheme. A simulation experiment is given in Section 5. Finally, Section 6 makes a conclusion.

2. Problem Statement

In this section, the UAV model is described for later investigation firstly. Then, we introduce the time-varying formation tracking problem of multi-UAV system. Finally, a hysteretic quantizer and several preliminaries are stated.

2.1. Problem Description. Consider a multi-UAV system which contains N UAVs. The UAVs are assumed to be equipped with standard autopilots and maintain a certain altitude during formation tracking based on practical applications. Since the UAVs have typically nonholonomic constraints, the kinematic model of the ith UAV is described as

$$\begin{bmatrix} \dot{x}_i \\ \dot{y}_i \\ \dot{\psi}_i \end{bmatrix} = \begin{bmatrix} \cos\psi_i \\ \sin\psi_i \\ 0 \end{bmatrix} v_i + \begin{bmatrix} 0 \\ 0 \\ 1 \end{bmatrix} w_i, \quad i = 1, \ldots, N, \tag{1}$$

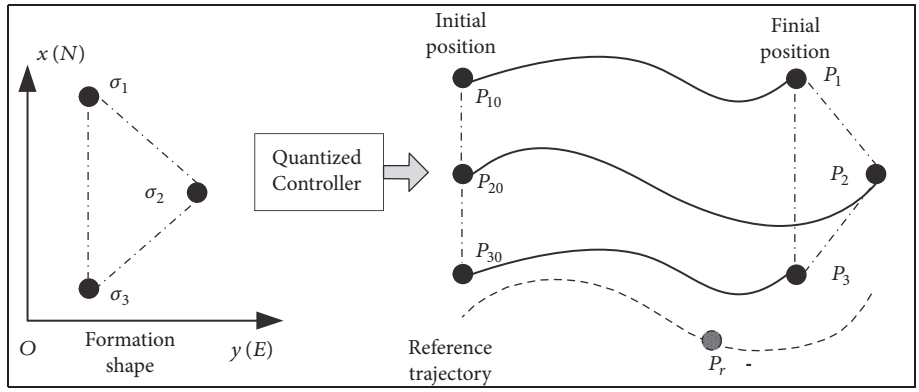

Figure 1: Formation tracking illustration.

where $(x_i, y_i)^T$ is the Cartesian position of the ith UAV, ψ_i is the orientation of the ith UAV, and v_i and w_i are the linear and angular velocities, respectively. Moreover, the autopilot model is described as

$$\begin{aligned} \dot{v}_i &= \frac{1}{\eta_{iv}} \left(q\left(v_i^u\right) - v_i \right) + d_{iv}(t), \\ \dot{w}_i &= \frac{1}{\eta_{iw}} \left(q\left(w_i^u\right) - w_i \right) + d_{iw}(t), \end{aligned} \tag{2}$$

where η_{iv} and η_{iw} are unknown positive parameters. $d_{iv}(t)$ and $d_{iw}(t)$ are time-varying disturbances with unknown bounds. $q(v_i^u)$ and $q(w_i^u)$ are quantized commanded linear and angular velocities with input signals v_i^u and w_i^u to be designed. In actual UAV control practice, the autopilot inputs, v_i^u and w_i^u, are computed from the information of the UAV kinematic model. From (2), it is shown that the autopilot outputs can change the linear and angular velocities in kinematic model. Thus, it achieves the control of UAV position and orientation.

The formation tracking process of multiple UAVs is illustrated in Figure 1. The three points represent three UAVs. With proper design of the quantized controller, the multi-UAV system can track the reference trajectory and maintain the desired formation shape. $P_r(t) = (x_r, y_r)^T$ and $\sigma_i(t) = (\sigma_{ix}, \sigma_{iy})^T$ represent the reference trajectory and relative position of the ith UAV in the formation shape for $i = 1, 2, 3$. $P_{i0} = (x_{i0}, y_{i0})^T$ and $P_i(t) = (x_i, y_i)^T$ represent its initial position and finial position. To avoid the weak point of leader failure in leader-follower structure, virtual structure is used for the formation topology structure. All the UAVs can get reference information from virtual leader. Through maintaining desired relative positions with virtual leader, the UAVs can form the desired formation shape. Therefore, the control objective is to design an adaptive controller $u_i = (v_i^u, w_i^u)^T$ where $i = 1, \ldots, N$ such that

(i) all the closed-loop signals are semiglobally finite-time bounded,

(ii) the N UAVs can track the reference trajectory $P_r(t)$ and form the desired formation shape with tracking errors converging to an adjustable small neighborhood of the origin in finite time.

There is a common assumption for the system.

Assumption 1. The reference trajectory $P_r(t)$, relative position $\sigma_i(t)$, and their first 2nd-order time derivatives are continuous and bounded.

Remark 2. It is always required for multi-UAV systems to execute various missions on the basis of time-varying formation shape. The formation shapes are changed through the adjustment of the parameter $\sigma_i(t)$. If $\sigma_i(t)$ is chosen to be constant, the formation shape will keep fixed.

2.2. Hysteretic Quantizer. In networked control systems, control signals are always quantized before being transmitted. The quantization effects may lead to worse performance or even instability. To reduce chattering, hysteretic quantizer is introduced and defined as

$$q(v(t)) = \begin{cases} u_j \operatorname{sign}(v), & \dfrac{u_j}{1+\delta} < |v| \le u_j, \ \dot{v} < 0, \text{ or} \\ & u_j < |v| \le \dfrac{u_j}{1-\delta}, \ \dot{v} > 0, \\ u_j (1+\delta) \operatorname{sign}(v), & u_j < |v| \le \dfrac{u_j}{1-\delta}, \ \dot{v} < 0, \text{ or} \\ & \dfrac{u_j}{1-\delta} < |v| \le \dfrac{u_j (1+\delta)}{1-\delta}, \ \dot{v} > 0, \\ 0, & 0 \le |v| < \dfrac{u_{\min}}{1+\delta}, \ \dot{v} < 0, \text{ or} \\ & \dfrac{u_{\min}}{1+\delta} \le |v| < u_{\min}, \ \dot{v} > 0, \\ q\left(v\left(t^-\right)\right), & \dot{v} = 0, \end{cases} \tag{3}$$

where $u_j = \rho^{1-j} u_{\min}$ $(j = 1, 2, \cdots)$, $0 < \rho < 1$, and $\delta = (1-\rho)/(1+\rho)$. $u_{\min}$ represents the dead-zone for $q(v(t))$.

Remark 3. The density constant $\rho \in (0, 1)$ is a quantization measurement. The smaller value of ρ means a coarser quantizer. The equation $\delta = (1-\rho)/(1+\rho)$ suggests that $q(v(t))$ has fewer quantization levels when δ is close to 1.

Researchers always use sector bound property to decompose the quantized signals into linear and nonlinear parts; i.e., $q(v) = v + \tau(v)$, where the nonlinear part $\tau(v)$ satisfies the inequality $|\tau(v)| \le \delta |v| + u_{\min}$ [13, 14]. Different

from the conventional quantization decomposition, a new decomposition method is used in this study as follows:

$$q(v) = \varsigma(v)\, v + \Delta(v), \tag{4}$$

where

$$\varsigma(v) = \begin{cases} \dfrac{q(v)}{v}, & q(v) \neq 0 \\ 1, & q(v) = 0, \end{cases}$$
$$\Delta(v) = \begin{cases} 0, & q(v) \neq 0 \\ -v, & q(v) = 0. \end{cases} \tag{5}$$

With the decomposition parts in (5), we can obtain that

$$\begin{aligned} (1-\delta)\, v \leqslant q(v) \leqslant (1+\delta)\, v, \quad q(v) > 0 \\ (1+\delta)\, v \leqslant q(v) \leqslant (1-\delta)\, v, \quad q(v) < 0, \end{aligned} \tag{6}$$

which indicates that

$$1 - \delta \leqslant \varsigma(v) \leqslant 1 + \delta. \tag{7}$$

In addition, we have $-u_{\min} \leqslant \Delta(v) \leqslant u_{\min}$ when $q(v) = 0$. Thus, it is obtained that

$$|\Delta(v)| \leqslant u_{\min}. \tag{8}$$

Remark 4. In the conventional decomposition, the nonlinear part $\tau(v)$ is regarded as a disturbance, which makes it a factor that leads to the tracking error. In addition, the bound of $\tau(v)$ depends on the control input. Thus, a restriction is required for the control input in [13]. This restriction is released in [14] by using the backstepping technique. However, the proposed stabilization control approach in [14] cannot be applied to trajectory tracking problem. With the new decomposition in this study, the quantization effects can be eliminated and the additional restrictions are released.

2.3. Mathematical Preliminaries. Not only steady performance, but also transient performance is required to be considered in finite-time controller design. In finite-time control systems, the tracking errors of the system trajectories are required to reach the desired boundaries in finite time. Therefore, several lemmas are stated for the finite-time controller design.

Lemma 5 (see [23]). *For $z_i \in \mathbb{R}$ $(i = 1, \ldots, n)$ and $\iota \in (0,1)$, the inequality $(|z_1| + \cdots + |z_n|)^{\iota} \leqslant |z_1|^{\iota} + \cdots + |z_n|^{\iota}$ holds.*

Lemma 6 (see [24]). *For any variables $d_1, d_2 \in \mathbb{R}$, an inequality holds as follows:*

$$\begin{aligned} |d_1|^{h_1} |d_2|^{h_2} \leqslant \frac{h_1}{h_1+h_2} s |d_1|^{h_1+h_2} \\ + \frac{h_2}{h_1+h_2} s^{-h_1/h_2} |d_2|^{h_1+h_2}, \end{aligned} \tag{9}$$

where h_1, h_2, and s can be chosen as any positive real constants.

Definition 7. Consider a nonlinear system $\dot{x} = f(x,u)$, where $x \in \mathbb{R}^n$ and $u \in \mathbb{R}^m$ are system state and input, respectively. $f : \mathcal{U} \to \mathbb{R}^n$ is continuously differentiable on an open neighborhood $\mathcal{U}$ of the origin with $f(0,0) = 0$. Suppose that, for any initial condition $x(t_0) = x_0$, there exist $\epsilon > 0$ and a settling time $0 < T(x_0, \epsilon) < \infty$ such that $\|x(t)\| \leqslant \epsilon$ when $t \geqslant t_0 + T$. Then, the origin of the nonlinear system $\dot{x} = f(x,u)$ is semiglobal practical finite-time stability.

Lemma 8 (see [25]). *Consider the system $\dot{x} = f(x,u)$ in Definition 7. If there exists a continuously differentiable function $V(x) : \mathcal{U} \to \mathbb{R}$ which is positive definite on $\mathcal{U}$ with $V(0) = 0$ and the inequality $\dot{V}(x) \leqslant -\phi V^{\varpi}(x) + \varphi$ holds, where the real numbers $\varpi \in (0,1)$, $\phi > 0$, and $0 < \varphi < \infty$, the trajectory of this system is semiglobal practical finite-time stability. In addition, the finite convergence time T satisfies that $T \leqslant V^{1-\varpi}(x(0))/(1-\varpi)\theta\phi$ where $\theta \in (0,1)$ is a design parameter.*

3. Adaptive Finite-Time Controller Design

The adaptive controller design is based on finite-time Lyapunov stability theory and backstepping technique. The design process contains three steps. Firstly, a transverse function method is used to remove the nonholonomic constraints in the kinematic model of UAVs. Secondly, we design the virtual control signals of linear and angular velocities based on the transformed coordinate. Finally, the actual control signals are designed for the autopilot model.

3.1. Coordinate Transformation. Considering there exist difficulties in the nonholonomic constraints of UAV kinematic model, a coordinate transformation is used to the kinematic model by using transverse function method. The transformation is established as follows:

$$\begin{bmatrix} \overline{x}_i \\ \overline{y}_i \end{bmatrix} = \begin{bmatrix} x_i \\ y_i \end{bmatrix} + Q(\overline{\psi}_i) \begin{bmatrix} h_{i1}(\zeta_i) \\ h_{i2}(\zeta_i) \end{bmatrix},$$
$$\overline{\psi}_i = \psi_i - h_{i3}, \tag{10}$$

where $(\overline{x}_i, \overline{y}_i)$ is the transformed position of the ith UAV, $\overline{\psi}_i$ is the transformed orientation, and

$$Q(\overline{\psi}_i) = \begin{bmatrix} \cos(\overline{\psi}_i) & -\sin(\overline{\psi}_i) \\ \sin(\overline{\psi}_i) & \cos(\overline{\psi}_i) \end{bmatrix}. \tag{11}$$

Besides, $h_{i1}(\zeta_i), h_{i2}(\zeta_i)$, and $h_{i3}(\zeta_i)$ are functions of variable ζ_i and defined as

$$\begin{aligned} h_{i1}(\zeta_i) &= e_{i1} \sin(\zeta_i) \frac{\sin(h_{i3})}{h_{i3}}, \\ h_{i2}(\zeta_i) &= e_{i1} \sin(\zeta_i) \frac{1-\cos(h_{i3})}{h_{i3}}, \\ h_{i3}(\zeta_i) &= e_{i2} \cos(\zeta_i), \end{aligned} \tag{12}$$

where $e_{i1}, e_{i2} \in (0, \pi/2)$ are positive constants. Therefore, it is obtained that

$$\begin{aligned} |h_{i1}(\zeta_i)| &< e_{i1}, \\ |h_{i2}(\zeta_i)| &< e_{i1}, \\ |h_{i3}(\zeta_i)| &< e_{i2}, \end{aligned} \tag{13}$$

which further implies that

$$\begin{aligned} \left\|(\overline{x}_i - x_i), (\overline{y}_i - y_i)\right\| &\leqslant \sqrt{2e_{i1}^2}, \\ |\overline{\psi}_i - \psi_i| &\leqslant e_{i2}. \end{aligned} \tag{14}$$

Based on (12), differentiating (10) yields

$$\begin{aligned} \begin{bmatrix} \dot{\overline{x}}_i \\ \dot{\overline{y}}_i \end{bmatrix} &= R_i \begin{bmatrix} v_i \\ \dot{\zeta}_i \end{bmatrix} \\ &\quad + \frac{\partial Q(\overline{\psi}_i)}{\partial \overline{\psi}_i} \begin{bmatrix} h_{i1}(\zeta_i) \\ h_{i2}(\zeta_i) \end{bmatrix} \left(w_i - \frac{\partial h_{i3}(\zeta_i)}{\partial \zeta_i} \dot{\zeta}_i \right), \\ \dot{\overline{\psi}}_i &= w_i - \frac{\partial h_{i3}(\zeta_i)}{\partial \zeta_i} \dot{\zeta}_i, \end{aligned} \tag{15}$$

where

$$R_i = \begin{bmatrix} \begin{pmatrix} \cos(\psi_i) \\ \sin(\psi_i) \end{pmatrix} & Q(\overline{\psi}_i) \begin{pmatrix} \dfrac{\partial h_{i1}(\zeta_i)}{\partial \zeta_i} \\ \dfrac{\partial h_{i2}(\zeta_i)}{\partial \zeta_i} \end{pmatrix} \end{bmatrix}. \tag{16}$$

3.2. Control Design of Kinematic Model. The trajectory tracking errors of the ith UAV are defined as

$$\begin{aligned} z_{ix} &= \overline{x}_i - \sigma_{ix} - x_r, \\ z_{iy} &= \overline{y}_i - \sigma_{iy} - y_r, \\ z_{i\psi} &= \overline{\psi}_i - \psi_r, \end{aligned} \tag{17}$$

where $\psi_r = \arctan(\dot{y}_r/\dot{x}_r)$.

Let $sig^a = \text{sign}(x)|x|^a$ with $a > 0$ and $x \in \mathbb{R}$. Then, we design the first virtual controller as

$$\begin{aligned} \begin{bmatrix} \alpha_{iv} \\ \dot{\zeta}_i \end{bmatrix} &= R_i^{-1} \left(-k_{i1} \begin{bmatrix} z_{ix} \\ z_{iy} \end{bmatrix} - g_{i1} \begin{bmatrix} sig^q(z_{ix}) \\ sig^q(z_{iy}) \end{bmatrix} \right. \\ &\quad + \frac{\partial Q(\overline{\psi}_i)}{\partial \overline{\psi}_i} \\ &\quad \cdot \begin{bmatrix} h_{i1}(\zeta_i) \\ h_{i2}(\zeta_i) \end{bmatrix} \left(k_{i2} z_{i\psi} + g_{i2} \left(sig^q(z_{i\psi}) \right) - \dot{\psi}_r \right) \\ &\quad \left. + \begin{bmatrix} \dot{x}_r + \dot{\sigma}_{ix} \\ \dot{y}_r + \dot{\sigma}_{iy} \end{bmatrix} \right), \\ \alpha_{iw} &= -k_{i2} z_{i\psi} - g_{i2} \left(sig^q(z_{i\psi}) \right) + \frac{\partial h_{i3}(\zeta_i)}{\partial \zeta_i} \dot{\zeta}_i + \dot{\psi}_r, \end{aligned} \tag{18}$$

where k_{i1}, k_{i2}, g_{i1}, and g_{i2} are positive parameters, $0 < q < 1$.

Define a Lyapunov function as

$$V_{i1} = \frac{1}{2} \left(z_{ix}^2 + z_{iy}^2 + z_{i\psi}^2 \right), \tag{19}$$

whose time derivative is calculated as

$$\begin{aligned} \dot{V}_{i1} &= -k_{i1} \left(z_{ix}^2 + z_{iy}^2 \right) - g_{i1} \begin{bmatrix} z_{ix} & z_{iy} \end{bmatrix} \begin{bmatrix} sig^q(z_{ix}) \\ sig^q(z_{iy}) \end{bmatrix} \\ &\quad - k_{i2} z_{i\psi}^2 - g_{i2} z_{i\psi} sig^q(z_{i\psi}) + \Upsilon_i (v_i - \alpha_{iv}) \\ &\quad + \Psi_i (w_i - \alpha_{iw}), \end{aligned} \tag{20}$$

where

$$\begin{aligned} \Upsilon_i &= z_{ix} \cos\psi_i + z_{iy} \sin\psi_i, \\ \Psi_i &= \begin{bmatrix} z_{ix} & z_{iy} \end{bmatrix} \frac{\partial Q(\overline{\psi}_i)}{\partial \overline{\psi}_i} \begin{bmatrix} h_{i1}(\zeta_i) \\ h_{i2}(\zeta_i) \end{bmatrix} + z_{i\psi}. \end{aligned} \tag{21}$$

3.3. Control Design of Autopilot Model. With the virtual control signals α_{iv} and α_{iw}, we define the errors of linear and angular velocities as

$$\begin{aligned} z_{iv} &= v_i - \alpha_{iv}, \\ z_{iw} &= w_i - \alpha_{iw}. \end{aligned} \tag{22}$$

Using (2) and (18), the time derivative of (22) can be expressed as

$$\begin{aligned} \dot{z}_{iv} &= \dot{v}_i - \dot{\alpha}_{iv} = \frac{1}{\eta_{iv}} \left(q(v_i^u) - v_i \right) + d_{iv} - \dot{\alpha}_{iv}, \\ \dot{z}_{iw} &= \dot{w}_i - \dot{\alpha}_{iw} = \frac{1}{\eta_{iw}} \left(q(w_i^u) - w_i \right) + d_{iw} - \dot{\alpha}_{iw}. \end{aligned} \tag{23}$$

For the ith UAV, there exist unknown positive constants $\overline{d}_{iv}$ and $\overline{d}_{iw}$ such that $|d_{iv}(t)| \leqslant \overline{d}_{iv}$ and $|d_{iw}(t)| \leqslant \overline{d}_{iw}$ when $\forall t > 0$. Then, the quantized controller is established as follows:

$$\begin{aligned} v_i^u &= \beta_{iv}^T v_{ic}, \\ w_i^u &= \beta_{iw}^T w_{ic}, \\ \beta_{iv} &= \begin{bmatrix} \beta_{iv1} & \beta_{iv2} & \beta_{iv3} \end{bmatrix}^T \\ &= \begin{bmatrix} \dfrac{1}{\widehat{\vartheta}_{iv}(1 - \delta_{iv})} & \dfrac{u_{\min}^{iv}}{1 - \delta_{iv}} & \dfrac{1}{\widehat{\vartheta}_{iv}(1 - \delta_{iv})} \end{bmatrix}^T, \\ v_{ic} &= \begin{bmatrix} v_{ic1} & v_{ic2} & v_{ic3} \end{bmatrix}^T \\ &= \begin{bmatrix} -\dfrac{z_{iv}\kappa_{iv}^2}{\sqrt{z_{iv}^2\kappa_{iv}^2 + \xi_{iv1}^2}} & -\dfrac{z_{iv}}{\sqrt{z_{iv}^2 + \xi_{iv2}^2}} & -\dfrac{z_{iv}\widehat{d}_{iv}^2}{\sqrt{z_{iv}^2\widehat{d}_{iv}^2 + \xi_{iv3}^2}} \end{bmatrix}^T, \end{aligned}$$

$$\beta_{iw} = \left[\beta_{iw1} \;\; \beta_{iw2} \;\; \beta_{iw3}^T\right] = \left[\frac{1}{\widehat{\vartheta}_{iw}(1-\delta_{iw})} \;\; \frac{u_{\min}^{iw}}{1-\delta_{iw}} \;\; \frac{1}{\widehat{\vartheta}_{iw}(1-\delta_{iw})}\right]^T,$$
$$w_{ic} = \left[w_{ic1} \;\; w_{ic2} \;\; w_{ic3}\right]^T = \left[-\frac{z_{iw}\kappa_{iw}^2}{\sqrt{z_{iw}^2\kappa_{iw}^2+\xi_{iw1}^2}} \;\; -\frac{z_{iw}}{\sqrt{z_{iw}^2+\xi_{iw2}^2}} \;\; -\frac{z_{iw}\widehat{d}_{iw}^2}{\sqrt{z_{iw}^2\widehat{d}_{iw}^2+\xi_{iw3}^2}}\right]^T, \tag{24}$$

where $\widehat{\vartheta}_{iv}$, $\widehat{\vartheta}_{iw}$, $\widehat{d}_{iv}$, and $\widehat{d}_{iw}$ are the estimations of the unknown positive parameters $\vartheta_{iv} = 1/\eta_{iv}$, $\vartheta_{iw} = 1/\eta_{iw}$, $\overline{d}_{iv}$, and $\overline{d}_{iw}$, respectively. $\xi_a (a = iv1, iv2, iv3, iw1, iw2, iw3)$ are positive design parameters. $u_{\min}^{iv}$ and δ_{iv} are the designed parameters of the quantizer $q(v_i^u)$ of linear velocity. $u_{\min}^{iw}$ and δ_{iw} are the designed parameters of the quantizer $q(w_i^u)$ of angular velocity. The parameters κ_{iv} and κ_{iw} are defined as

$$\kappa_{iv} = -\widehat{\vartheta}_{iv}v_i - \dot{\alpha}_{iv} + \Upsilon_i + k_{i3}z_{iv} + g_{i3}sig^q(z_{iv}),$$
$$\kappa_{iw} = -\widehat{\vartheta}_{iw}w_i - \dot{\alpha}_{iw} + \Psi_i + k_{i4}z_{iw} + g_{i4}sig^q(z_{iw}), \tag{25}$$

where k_{i3}, k_{i4}, g_{i3}, and g_{i4} are positive constants. Relatively, the parameter update laws are designed as

$$\dot{\widehat{\vartheta}}_{iv} = Proj\left\{-\gamma_{iv}\frac{z_{iv}^2\kappa_{iv}^2}{\widehat{\vartheta}_{iv}\sqrt{z_{iv}^2\kappa_{iv}^2+\xi_{iv1}^2}} - \gamma_{iv}\frac{z_{iv}^2\widehat{d}_{iv}^2}{\widehat{\vartheta}_{iv}\sqrt{z_{iv}^2\widehat{d}_{iv}^2+\xi_{iv3}^2}} - \gamma_{iv}z_{iv}v_i - \mu_i\widehat{\vartheta}_{iv}\right\},$$
$$\dot{\widehat{\vartheta}}_{iw} = Proj\left\{-\gamma_{iw}\frac{z_{iw}^2\kappa_{iw}^2}{\widehat{\vartheta}_{iw}\sqrt{z_{iw}^2\kappa_{iw}^2+\xi_{iw1}^2}} - \gamma_{iw}\frac{z_{iw}^2\widehat{d}_{iw}^2}{\widehat{\vartheta}_{iw}\sqrt{z_{iw}^2\widehat{d}_{iw}^2+\xi_{iw3}^2}} - \gamma_{iw}z_{iw}w_i - \mu_i\widehat{\vartheta}_{iw}\right\},$$
$$\dot{\widehat{d}}_{iv} = Proj\left\{-\varrho_{iv}|z_{iv}| - \mu_i\widehat{d}_{iv}\right\},$$
$$\dot{\widehat{d}}_{iw} = Proj\left\{-\varrho_{iw}|z_{iw}| - \mu_i\widehat{d}_{iw}\right\}, \tag{26}$$

where μ_i, γ_{iv}, γ_{iw}, ϱ_{iv}, and ϱ_{iw} are positive design constants. To ensure that $\widehat{\vartheta}_{iv}$, $\widehat{\vartheta}_{iw}$, $\widehat{d}_{iv}$, and $\widehat{d}_{iw}$ are greater than zero, the projection operator $Proj\{\cdot\}$ is utilized in the calculation of parameter update laws. It is worth mentioning that projection operator has a useful property; that is, it satisfies $-(1/\gamma)\widetilde{\vartheta}Proj\{\lambda\} \leqslant -(1/\gamma)\widetilde{\vartheta}\lambda$. It will be utilized in the following analysis.

4. Stability Analysis

Now, we present the following theorem to summarize the analysis in this study.

Theorem 9. *Consider a multi-UAV system consisting of UAVs which are described by nonholonomic kinematic model (1), autopilot model (2), and hysteretic quantizer (3). Under the adaptive controller (24), parameter update law (26), and the condition that Assumption 1 holds, the finite-time formation tracking of multi-UAV system can be achieved such that*

(i) all the signals in the closed-loop system are semiglobally finite-time bounded,

(ii) the formation tracking errors can converge to a small neighborhood of the origin in finite time.

Proof. To analyze the stability of the overall closed-loop system, a Lyapunov function is defined as

$$V_i = V_{i1} + \frac{1}{2}z_{iv}^2 + \frac{1}{2}z_{iw}^2 + \frac{1}{2\gamma_{iv}}\widetilde{\vartheta}_{iv}^2 + \frac{1}{2\gamma_{iw}}\widetilde{\vartheta}_{iw}^2 + \frac{1}{2\varrho_{iv}}\widetilde{d}_{iv}^2 + \frac{1}{2\varrho_{iw}}\widetilde{d}_{iw}^2, \tag{27}$$

where $\widetilde{\vartheta}_{iv} = \vartheta_{iv} - \widehat{\vartheta}_{iv}$, $\widetilde{\vartheta}_{iw} = \vartheta_{iw} - \widehat{\vartheta}_{iw}$, $\widetilde{d}_{iv} = \overline{d}_{iv} - \widehat{d}_{iv}$, and $\widetilde{d}_{iw} = \overline{d}_{iw} - \widehat{d}_{iw}$.

Since β_{iv1} and β_{iv3} are greater than zero according to $\widehat{\vartheta}_{iv} > 0$, it can be checked that

$$\beta_{iv}^T v_{ic} z_{iv} = -\beta_{iv1}\frac{z_{iv}^2\kappa_{iv}^2}{\sqrt{z_{iv}^2\kappa_{iv}^2+\xi_{iv1}^2}} - \beta_{iv2}\frac{z_{iv}^2}{\sqrt{z_{iv}^2+\xi_{iv2}^2}} - \beta_{iv3}\frac{z_{iv}^2\widehat{d}_{iv}^2}{\sqrt{z_{iv}^2\widehat{d}_{iv}^2+\xi_{iv3}^2}} \leqslant 0. \tag{28}$$

By taking similar procedure, we can prove that $\beta_{iw}^T w_{ic} z_{iw} \leqslant 0$. Since the inequality $0 \leqslant |b_1| - b_1^2/\sqrt{b_1^2+b_2^2} \leqslant b_2$ holds when $b_2 \geqslant 0$, we have

$$z_{iv}\kappa_{iv} - \frac{z_{iv}^2\kappa_{iv}^2}{\sqrt{z_{iv}^2\kappa_{iv}^2+\xi_{iv1}^2}} \leqslant \xi_{iv1},$$
$$|z_{iv}| - \frac{z_{iv}^2}{\sqrt{z_{iv}^2+\xi_{iv2}^2}} \leqslant \xi_{iv2}, \tag{29}$$
$$\widehat{d}_{iv}|z_{iv}| - \frac{z_{iv}^2\widehat{d}_{iv}^2}{\sqrt{z_{iv}^2\widehat{d}_{iv}^2+\xi_{iv3}^2}} \leqslant \xi_{iv3}.$$

Taking (4), (23)-(25), and (29) into consideration, we can obtain that

$$z_{iv}\dot{z}_{iv} = z_{iv}\left(\vartheta_{iv}\left(q\left(v_i^u\right) - v_i\right) + d_{iv}(t) - \dot{\alpha}_{iv}\right) = z_{iv}\left(\vartheta_{iv}\left(\varsigma_{iv}\left(v_i^u\right)\beta_{iv}^T v_{ic} + \Delta_{iv}\left(v_i^u\right) - v_i\right) + d_{iv}(t)\right.$$

$$
\begin{aligned}
&-\dot{\alpha}_{iv}\Big) \leqslant z_{iv}\Big(\vartheta_{iv}\left(1-\delta_{iv}\right)\beta_{iv1}v_{ic1}\\
&+\vartheta_{iv}\left(1-\delta_{iv}\right)\beta_{iv2}v_{ic2}+\vartheta_{iv}\left(1-\delta_{iv}\right)\beta_{iv3}v_{ic3}\\
&+\vartheta_{iv}u_{\min}^{iv}-\vartheta_{iv}v_i+d_{iv}\left(t\right)-\dot{\alpha}_{iv}\Big) \leqslant z_{iv}\kappa_{iv}\\
&-\frac{z_{iv}^2\kappa_{iv}^2}{\sqrt{z_{iv}^2\kappa_{iv}^2+\xi_{iv1}^2}}+\vartheta_{iv}u_{\min}^{iv}\left|z_{iv}\right|-\vartheta_{iv}\frac{u_{\min}^{iv}z_{iv}^2}{\sqrt{z_{iv}^2+\xi_{iv2}^2}}\\
&+\widehat{d}_{iv}\left|z_{iv}\right|-\frac{z_{iv}^2\widehat{d}_{iv}^2}{\sqrt{z_{iv}^2\widehat{d}_{iv}^2+\xi_{iv3}^2}}+\widetilde{d}_{iv}\left|z_{iv}\right|-k_{i3}z_{iv}^2\\
&-g_{i3}z_{iv}sig^q\left(z_{iv}\right)-\widetilde{\vartheta}_{iv}\Bigg(z_{iv}v_i+\frac{z_{iv}^2\kappa_{iv}^2}{\widehat{\vartheta}_{iv}\sqrt{z_{iv}^2\kappa_{iv}^2+\xi_{iv1}^2}}\\
&+\frac{z_{iv}^2\widehat{d}_{iv}^2}{\widehat{\vartheta}_{iv}\sqrt{z_{iv}^2\widehat{d}_{iv}^2+\xi_{iv3}^2}}\Bigg)-\left[z_{ix}\quad z_{iy}\right]\Upsilon_i z_{iv} \leqslant \xi_{iv1}\\
&+\vartheta_{iv}u_{\min}^{iv}\xi_{iv2}+\xi_{iv3}+\widetilde{d}_{iv}\left|z_{iv}\right|-g_{i3}z_{iv}sig^q\left(z_{iv}\right)\\
&-\widetilde{\vartheta}_{iv}\Bigg(z_{iv}v_i+\frac{z_{iv}^2\kappa_{iv}^2}{\widehat{\vartheta}_{iv}\sqrt{z_{iv}^2\kappa_{iv}^2+\xi_{iv1}^2}}\\
&+\frac{z_{iv}^2\widehat{d}_{iv}^2}{\widehat{\vartheta}_{iv}\sqrt{z_{iv}^2\widehat{d}_{iv}^2+\xi_{iv3}^2}}\Bigg)-k_{i3}z_{iv}^2-\Upsilon_i z_{iv}.
\end{aligned}
\tag{30}
$$

Similarly, the following equation is obtained:

$$
\begin{aligned}
z_{iw}\dot{z}_{iw} &= z_{iw}\left(\vartheta_{iw}\left(q\left(w_i^u\right)-w_i\right)+d_{iw}-\dot{\alpha}_{iw}\right) \leqslant \xi_{iw1}\\
&+\vartheta_{iw}u_{\min}^{iw}\xi_{iw2}+\xi_{iv3}+\widetilde{d}_{iw}\left|z_{iw}\right|-g_{i4}z_{iw}sig^q\left(z_{iw}\right)\\
&-\widetilde{\vartheta}_{iw}\Bigg(z_{iw}w_i+\frac{z_{iw}^2\kappa_{iw}^2}{\widehat{\vartheta}_{iw}\sqrt{z_{iw}^2\kappa_{iw}^2+\xi_{iw1}^2}}\\
&+\frac{z_{iw}^2\widehat{d}_{iw}^2}{\widehat{\vartheta}_{iw}\sqrt{z_{iw}^2\widehat{d}_{iw}^2+\xi_{iw3}^2}}\Bigg)-k_{i4}z_{iw}^2-\Psi_i z_{i\psi}.
\end{aligned}
\tag{31}
$$

Substituting (20), (30), and (31) into the time derivative of V_i, we can get that

$$
\begin{aligned}
\dot{V}_i &= \dot{V}_{i1}+z_{iv}\dot{z}_{iv}+z_{iw}\dot{z}_{iw}+\frac{1}{\gamma_{iv}}\widetilde{\vartheta}_{iv}\left(-\dot{\widehat{\vartheta}}_{iv}\right)\\
&+\frac{1}{\gamma_{iw}}\widetilde{\vartheta}_{iw}\left(-\dot{\widehat{\vartheta}}_{iw}\right)+\frac{1}{\varrho_{iv}}\widetilde{d}_{iv}\left(-\dot{\widehat{d}}_{iv}\right)\\
&+\frac{1}{\varrho_{iw}}\widetilde{d}_{iw}\left(-\dot{\widehat{d}}_{iw}\right)\\
&\leqslant -k_{i1}\left(z_{ix}^2+z_{iy}^2\right)-k_{i2}z_{i\psi}^2-k_{i3}z_{iv}^2-k_{i4}z_{iw}^2\\
&+\frac{\mu_i}{\gamma_{iv}}\widetilde{\vartheta}_{iv}\widehat{\vartheta}_{iv}+\frac{\mu_i}{\gamma_{iw}}\widetilde{\vartheta}_{iw}\widehat{\vartheta}_{iw}+\frac{\mu_i}{\varrho_{iv}}\widetilde{d}_{iv}\widehat{d}_{iv}+\frac{\mu_i}{\varrho_{iw}}\widetilde{d}_{iw}\widehat{d}_{iw}\\
&-g_{i1}\left(z_{ix}sig^q\left(z_{ix}\right)+z_{iy}sig^q\left(z_{iy}\right)\right)\\
&-g_{i2}z_{i\psi}sig^q\left(z_{i\psi}\right)-g_{i3}z_{iv}sig^q\left(z_{iv}\right)\\
&-g_{i4}z_{iw}sig^q\left(z_{iw}\right)+\xi_{iv1}+\vartheta_{iv}u_{\min}^{iv}\xi_{iv2}+\xi_{iv3}\\
&+\xi_{iw1}+\vartheta_{iw}u_{\min}^{iw}\xi_{iw2}+\xi_{iw3}.
\end{aligned}
\tag{32}
$$

According to Lemma 5, it can be checked that

$$
\begin{aligned}
&g_{i1}z_{ix}sig^q\left(z_{ix}\right)+g_{i1}z_{iy}sig^q\left(z_{iy}\right)+g_{i2}z_{i\psi}sig^q\left(z_{i\psi}\right)\\
&+g_{i3}z_{iv}sig^q\left(z_{iv}\right)+g_{i4}z_{iw}sig^q\left(z_{iw}\right) \geqslant g_i\Big(\left|z_{ix}\right|^{1+q}\\
&+\left|z_{iy}\right|^{1+q}+\left|z_{i\psi}\right|^{1+q}+\left|z_{iv}\right|^{1+q}+\left|z_{iw}\right|^{1+q}\Big) \geqslant g_i\Big(z_{ix}^2\\
&+z_{iy}^2+z_{i\psi}^2+z_{iv}^2+z_{iw}^2\Big)^{(1+q)/2},
\end{aligned}
\tag{33}
$$

where $g_i=\min(g_{i1},g_{i2},g_{i3},g_{i4},)$.

With the aid of Lemma 6, the parameters in (9) are set as $d_1=1$, $d_2=(\mu_i/2\gamma_{iv})\widetilde{\vartheta}_{iv}^2$, $h_1=(1-q)/2$, $h_2=(1+q)/2$, $s=((1-q)/2)\mathrm{e}^{((1+q)/(1-q))\ln((1+q)/2)}$. Then, it can be proved that

$$
\begin{aligned}
\left(\frac{\mu_i}{2\gamma_{iv}}\widetilde{\vartheta}_{iv}^2\right)^{(1+q)/2} &\leqslant \frac{1-q}{2}\mathrm{e}^{((1+q)/(1-q))\ln((1+q)/2)}\\
&+\frac{\mu_i}{2\gamma_{iv}}\widetilde{\vartheta}_{iv}^2.
\end{aligned}
\tag{34}
$$

Using (34) and noting that $\widetilde{\vartheta}_{iv}\widehat{\vartheta}_{iv} \leqslant (1/2)\vartheta_{iv}^2-(1/2)\widetilde{\vartheta}_{iv}^2$, we can obtain that

$$
\begin{aligned}
\frac{\mu_i}{\gamma_{iv}}\widetilde{\vartheta}_{iv}\widehat{\vartheta}_{iv} &= -\mu_i^{(1+q)/2}\left(\frac{1}{2\gamma_{iv}}\widetilde{\vartheta}_{iv}^2\right)^{(1+q)/2}+\frac{\mu_i}{\gamma_{iv}}\widetilde{\vartheta}_{iv}\widehat{\vartheta}_{iv}\\
&+\left(\frac{\mu_i}{2\gamma_{iv}}\widetilde{\vartheta}_{iv}^2\right)^{(1+q)/2}\\
&\leqslant -\mu_i^{(1+q)/2}\left(\frac{1}{2\gamma_{iv}}\widetilde{\vartheta}_{iv}^2\right)^{(1+q)/2}+\frac{\mu_i}{2\gamma_{iv}}\vartheta_{iv}^2\\
&+\frac{1-q}{2}\mathrm{e}^{((1+q)/(1-q))\ln((1+q)/2)}.
\end{aligned}
\tag{35}
$$

Taking the similar process of obtaining (35), we have

$$
\begin{aligned}
\frac{\mu_i}{\gamma_{iw}}\widetilde{\vartheta}_{iw}\widehat{\vartheta}_{iw} &\leqslant -\mu_i^{(1+q)/2}\left(\frac{1}{2\gamma_{iw}}\widetilde{\vartheta}_{iw}^2\right)^{(1+q)/2}+\frac{\mu_i}{2\gamma_{iw}}\vartheta_{iw}^2\\
&+\frac{1-q}{2}\mathrm{e}^{((1+q)/(1-q))\ln((1+q)/2)},
\end{aligned}
$$

$$\frac{\mu_i}{\varrho_{iv}}\widetilde{d}_{iv}\widehat{d}_{iv} \leqslant -\mu_i^{(1+q)/2}\left(\frac{1}{2\varrho_{iv}}\widetilde{d}_{iv}^2\right)^{(1+q)/2} + \frac{\mu_i}{2\varrho_{iv}}\overline{d}_{iv}^2 + \frac{1-q}{2}\mathrm{e}^{((1+q)/(1-q))\ln((1+q)/2)},$$

$$\frac{\mu_i}{\varrho_{iw}}\widetilde{d}_{iw}\widehat{d}_{iw} \leqslant -\mu_i^{(1+q)/2}\left(\frac{1}{2\varrho_{iw}}\widetilde{d}_{iw}^2\right)^{(1+q)/2} + \frac{\mu_i}{2\varrho_{iw}}\overline{d}_{iw}^2 + \frac{1-q}{2}\mathrm{e}^{((1+q)/(1-q))\ln((1+q)/2)}. \tag{36}$$

Substituting (33)-(36) into (32), it can be expressed as

$$\begin{aligned}\dot{V}_i \leqslant & -g_i\left(z_{ix}^2 + z_{iy}^2 + z_{i\psi}^2 + z_{iv}^2 + z_{iw}^2\right)^{(1+q)/2} \\ & - \mu_i^{(1+q)/2}\left(\frac{1}{2\gamma_{iv}}\widetilde{\vartheta}_{iv}^2\right)^{(1+q)/2} \\ & - \mu_i^{(1+q)/2}\left(\frac{1}{2\gamma_{iw}}\widetilde{\vartheta}_{iw}^2\right)^{(1+q)/2} \\ & - \mu_i^{(1+q)/2}\left(\frac{1}{2\varrho_{iv}}\widetilde{d}_{iv}^2\right)^{(1+q)/2} \\ & - \mu_i^{(1+q)/2}\left(\frac{1}{2\varrho_{iw}}\widetilde{d}_{iw}^2\right)^{(1+q)/2} + \frac{\mu_i}{2\gamma_{iv}}\vartheta_{iv}^2 + \frac{\mu_i}{2\gamma_{iw}}\vartheta_{iw}^2 \\ & + \frac{\mu_i}{2\varrho_{iv}}\overline{d}_{iv}^2 + \frac{\mu_i}{2\varrho_{iw}}\overline{d}_{iw}^2 \\ & + 2\left(1-q\right)\mathrm{e}^{((1+q)/(1-q))\ln((1+q)/2)} + \xi_{iv1} \\ & + \vartheta_{iv}u_{\min}^{iv}\xi_{iv2} + \xi_{iv3} + \xi_{iw1} + \vartheta_{iw}u_{\min}^{iw}\xi_{iw2} + \xi_{iw3}.\end{aligned} \tag{37}$$

Therefore, (37) can be rewritten as

$$\dot{V}_i \leqslant -l_i V_i^{(1+q)/2} + \Theta_i, \tag{38}$$

where $l_i = \min(g_i, \mu_i^{(1+q)/2})$, and the constant

$$\begin{aligned}\Theta_i = & \frac{\mu_i}{2\gamma_{iv}}\vartheta_{iv}^2 + \frac{\mu_i}{2\gamma_{iw}}\vartheta_{iw}^2 + \frac{\mu_i}{2\varrho_{iv}}\overline{d}_{iv}^2 + \frac{\mu_i}{2\varrho_{iw}}\overline{d}_{iw}^2 \\ & + 2\left(1-q\right)\mathrm{e}^{((1+q)/(1-q))\ln((1+q)/2)} + \xi_{iv1} \\ & + \vartheta_{iv}u_{\min}^{iv}\xi_{iv2} + \xi_{iv3} + \xi_{iw1} + \vartheta_{iw}u_{\min}^{iw}\xi_{iw2} + \xi_{iw3}.\end{aligned} \tag{39}$$

Based on Lemma 8 and (38)-(39), it is obtained that $V_i^{(1+q)/2}(t) \leqslant \Theta_i/(1-\theta)l_i$ when $t \geqslant T_i$ with the settling time

$$T_i = \frac{2V_i^{(1-q)/2}(0)}{(1-q)\theta l_i}. \tag{40}$$

Based on the former analysis, it is suggested that z_{ix}, z_{iy}, $z_{i\psi}$, z_{iv}, z_{iw}, $\widehat{\vartheta}_{iv}$, and $\widehat{\vartheta}_{iw}$ are semiglobal finite-time bounded. According to the boundedness of $P_r(t)$ and $\sigma_r(t)$, it is obtained that $\overline{x}_i$, $\overline{y}_i$, and $\overline{\psi}_i$ can keep semiglobal finite-time bound. Furthermore, the virtual control signals α_{iv}, α_{iw} and control signals v_i^u, w_i^u are bounded. Besides, according to the definition of V_i, it is obtained that $|z_{ix}(t)|$, $|z_{iy}(t)|$, and $|z_{i\psi}(t)|$ are all smaller than $(\Theta_i/(1-\theta)l_i)^{1/(1+q)}$ when $t \geqslant T_i$. Recalling (14) and (17), we can obtain that

$$\begin{aligned}\left|x_i - \delta_{ix} - x_r\right| &\leqslant \left|x_i - \overline{x}_i\right| + \left|\overline{x}_i - \delta_{ix} - x_r\right| \\ &\leqslant \sqrt{2}e_{i1} + \left|z_{ix}\right|, \\ \left|y_i - \delta_{iy} - y_r\right| &\leqslant \left|y_i - \overline{y}_i\right| + \left|\overline{y}_i - \delta_{iy} - y_r\right| \\ &\leqslant \sqrt{2}e_{i1} + \left|z_{iy}\right|, \\ \left|\psi_i - \psi_r\right| &\leqslant \left|\psi_i - \overline{\psi}_i\right| + \left|\overline{\psi}_i - \psi_r\right| \leqslant e_{i2} + \left|z_{i\psi}\right|.\end{aligned} \tag{41}$$

Therefore, it is proved that x_i, y_i, and ψ_i are semiglobal finite-time bounded. Based on the former analysis, it is suggested that all the closed-loop signals in the ith UAV are semiglobal finite-time bounded and the trajectory tracking errors of the ith UAV can converge to an adjustable small neighborhood of the origin in finite time. Taking the whole multi-UAV system into consideration, we define that $T = \max(T_1, \ldots, T_N)$. It can be concluded that all the signals in the system are semiglobally finite-time bounded and the tracking errors are steered to within an adjustable small neighborhood of the origin when $t \geqslant T$. □

Remark 10. Unlike using κ_{iv} and κ_{iw} in (25) as control signals in conventional backstepping controllers, we make a transformation (24) for κ_{iv} and κ_{iw}. The restrictions in [13, 14] are removed through utilizing the transformed signals as control signals. In addition, with the inequalities in (29), we can eliminate the quantization effects on the system stability based on the analysis of (30) and (31). Furthermore, there are no limitation on quantizer parameters, which allows a coarser quantization to be used in the controller.

Remark 11. Instead of estimating the real-time values of the time-varying disturbances $\widetilde{d}_{iv}$ and $\widetilde{d}_{iw}$, we choose to estimate the upper bounds of $\widetilde{d}_{iv}$ and $\widetilde{d}_{iw}$. For the requirement of finite-time convergence, the parameter update laws in (26) are designed to estimate the unknown parameters and upper bounds of disturbances. Due to the inequalities in (35) and (36), the control scheme can satisfy (38) and achieve the finite-time tracking.

5. Simulation

A simulation experiment is employed to demonstrate the effectiveness of the proposed control scheme. In the simulation experiment, we use a multi-UAV system which contains four UAVs. Our goal is to make the UAVs under the proposed control scheme achieve trajectory tracking in finite time. The reference trajectory is set as $(x_r, y_r) = (5t, 10\sin(0.2t))$. A time-varying formation shape is designed with the initial positions and relative positions in the formation of the UAVs

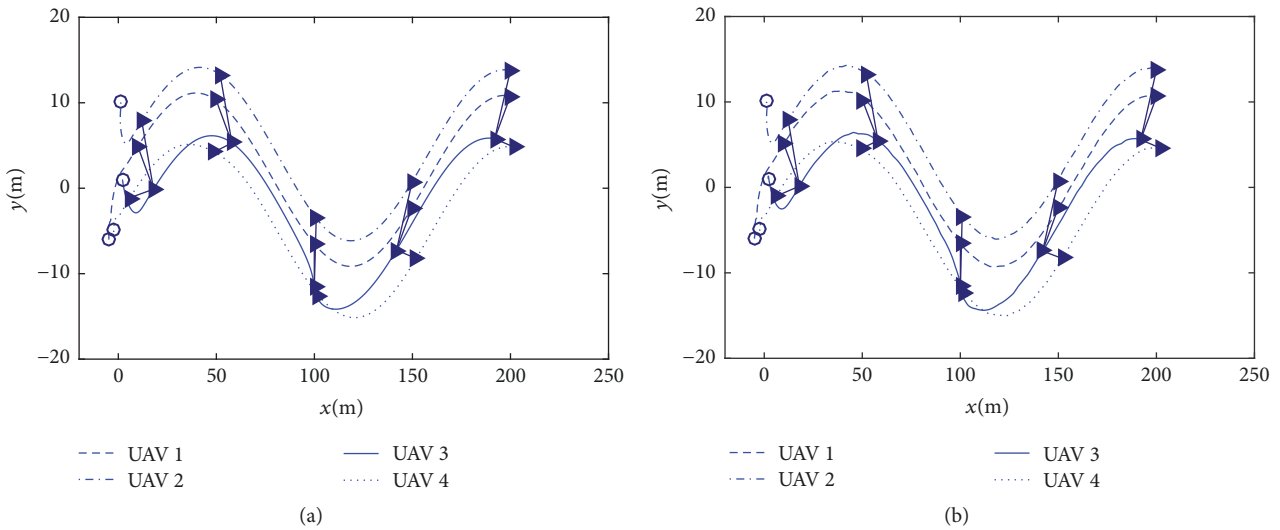

Figure 2: Formation trajectories. (a) the multi-UAV system with hysteretic quantizer (3), (b) the multi-UAV system with logarithmic quantizer (42).

Table 1: Initial and relative positions of the UAVs.

	Initial position	Relative position
UAV 1	$(-5, -6)$	$(0, 1)$
UAV 2	$(1, 10)$	$(-\tanh(0.5(t-20))-1, 4)$
UAV 3	$(2, 1)$	$(-8\tanh(0.5(t-20)), -4)$
UAV 4	$(-2.5, -5)$	$(3\tanh(0.5(t-20))-1, -5)$

being listed in Table 1. The initial linear and angular velocities of the UAVs are totally set as $v_i = 0m/s, w_i = 0rad/s$ for $i = 1, \ldots, 4$.

The kinematic and dynamic models of UAVs are described by (1) and (2). The unknown parameters of the autopilots are set as $\eta_{iv} = 0.8, \eta_{iw} = 1$. The unknown disturbances in the autopilots are given by $d_{iv}(t) = 0.15\sin(0.5t)$ and $d_{iw}(t) = 0.05\cos(0.75t)$. These values of unknown parameters and disturbances are used only for simulation and are unknown in controller design. The design parameters of hysteretic quantizers are defined as $\delta_{iv} = \delta_{iw} = 0.3$, $u^{iv}_{\min} = u^{iw}_{\min} = 0.02$. We choose the controller parameters as $k_{ij} = g_{ij} = 5$ $(i, j = 1, \ldots, 4)$, $q = 1/2$, $\gamma_{iv} = \gamma_{iw} = 1$, $\varrho_{iv} = \varrho_{iw} = 2$, and $\mu_i = 16$. The initial estimates of the adaptive parameters are chosen as $\widehat{\theta}_{iv}(0) = 3$, $\widehat{\theta}_{iw}(0) = 2$, $\widehat{d}_{iv}(0) = 0.5$, and $\widehat{d}_{iw}(0) = 0.2$.

In traditional quantized control schemes of continuous-time systems, chattering may occur in the quantized signals when the signals are processed by logarithmic quantizer. It is not desirable in the network since the transmission of signal chattering requires infinite bandwidth. To prove that the hysteretic quantizer (3) can reduce signal chattering, we also consider the same situation as above with the difference being the signal quantization. In this situation, the control input signals are processed by logarithmic quantizer instead of hysteretic quantizer. The logarithmic quantizer is defined as follows [12]:

$$Q_l(v) = \begin{cases} \rho_l^j u_{l,\min}, & \dfrac{\rho_l^j u_{l,\min}}{1+\delta_l} \le v < \dfrac{\rho_l^j u_{l,\min}}{1-\delta_l}, \quad j = 0, \pm 1, \pm 2, \ldots, \\ 0, & v = 0, \\ -Q(-v), & v < 0, \end{cases} \tag{42}$$

where quantization density $\rho_l \in (0, 1)$, $\delta_l = (1-\rho_l)/(1+\rho_l)$, and scaling parameter $u_{l,\min} > 0$. Here, we set $u_{l,\min} = 0.2$ and $\delta_l = 0.3$ for the logarithmic quantizer (42) used in the multi-UAV system.

The simulation results of the two situations are shown in Figures 2–8. From the formation trajectories in Figure 2, it is shown that the multi-UAV systems can both achieve the formation tracking fast and smoothly. However, some differences can be still observed from the tracking errors of all the UAVs given in Figures 3 and 4. As depicted in Figure 3, the UAVs with hysteretic quantizer (3) can reach the desired trajectories within the settling time $T = 1.57s$ and maintain high accuracy in steady performance. Figure 4 shows that slight oscillations and biases exist in the tracking errors of the multi-UAV system with logarithmic quantizer (42). Figure 5 shows the typical quantized input signals of the UAVs, i.e., $q(v_1^u)$ of the first UAV and $q(w_2^u)$ of the second UAV. These signals are processed by hysteretic quantizer (3), and signal chattering is highly reduced by observing the details of $q(v_1^u)$ and $q(w_2^u)$ in Figure 5. It shows that the input signals are simplified by hysteretic quantizer in favor of communication. The quantized input signals $Q_l(v_1^u)$ and $Q_l(w_2^u)$ are depicted in Figure 6 for the multi-UAV system with logarithmic quantizer (42). As the details of $Q_l(v_1^u)$ and $Q_l(w_2^u)$ show in Figure 6, signal chattering occurs during the control procedure. It is worth mentioning that

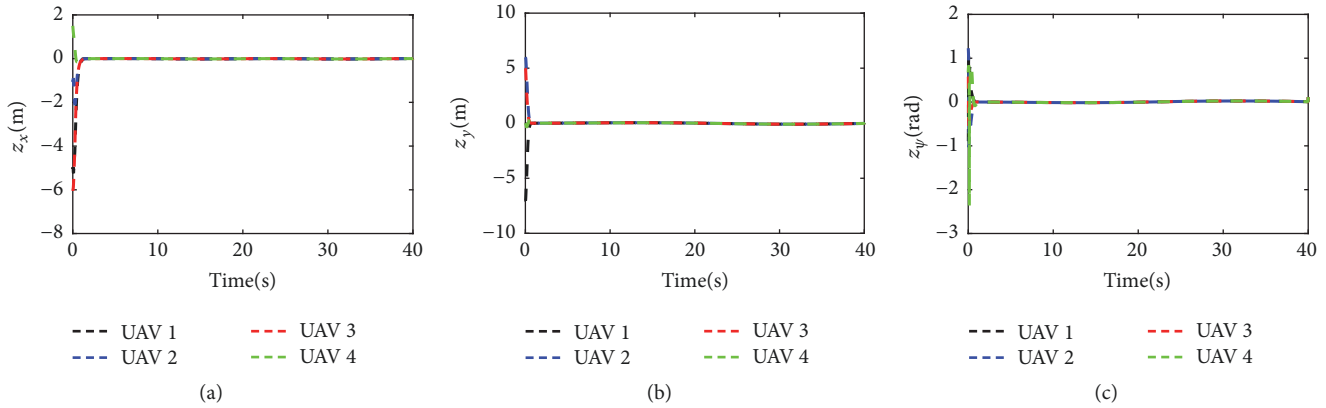

FIGURE 3: Tracking errors of the multi-UAV system with hysteretic quantizer (3). (a) z_x, (b) z_y, (c) z_ψ.

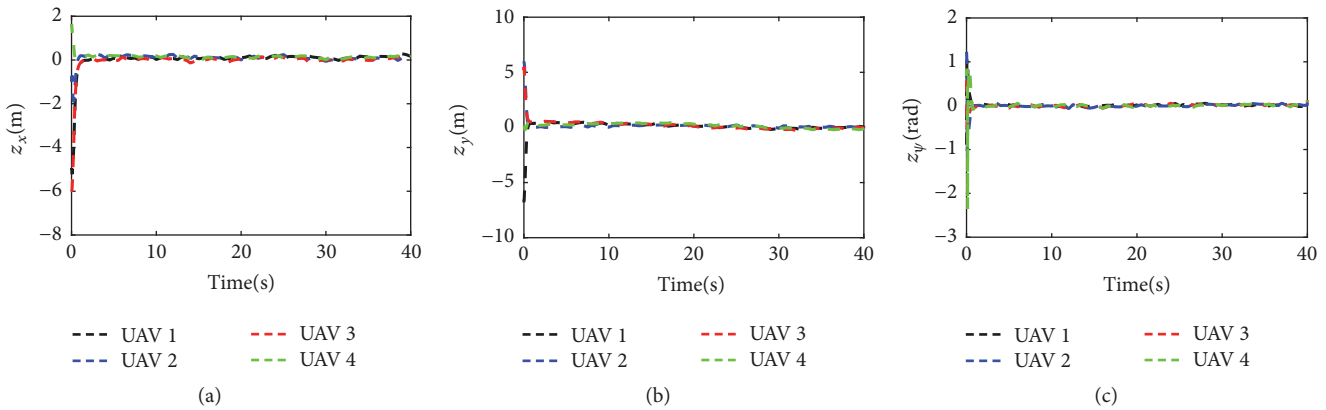

FIGURE 4: Tracking errors of the multi-UAV system with logarithmic quantizer (42). (a) z_x, (b) z_y, (c) z_ψ.

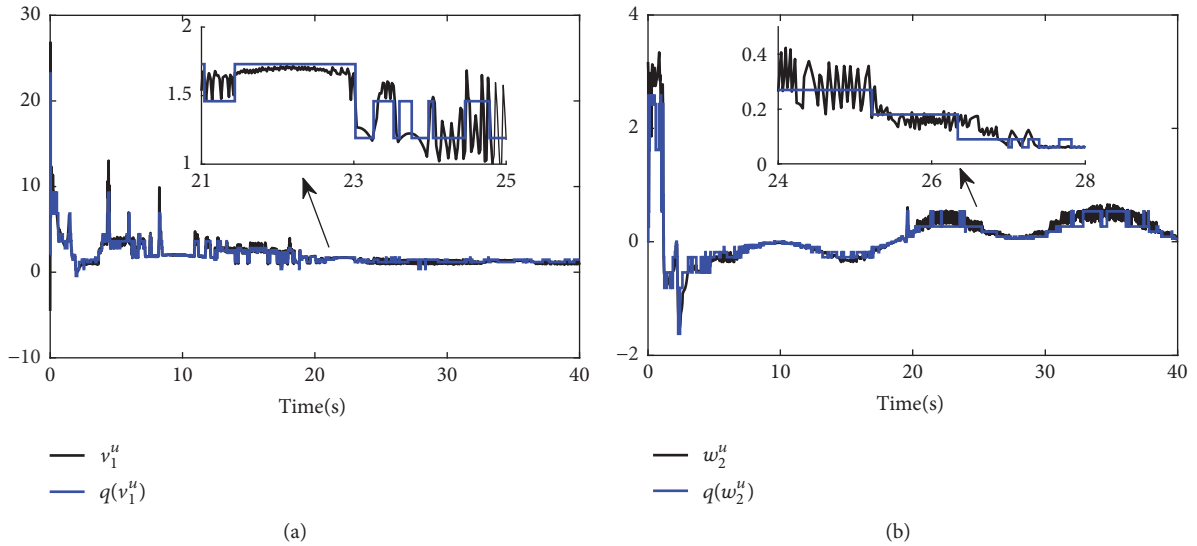

FIGURE 5: Quantized input in the multi-UAV system with hysteretic quantizer (3). (a) $q(v_1^u)$ of the first UAV, (b) $q(w_2^u)$ of the second UAV.

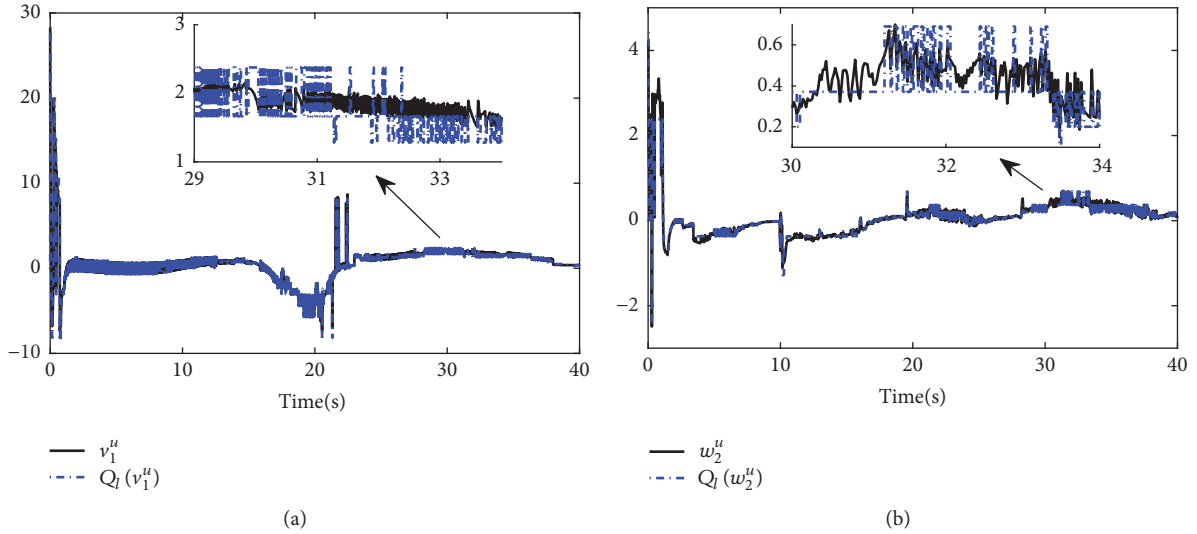

FIGURE 6: Quantized input in the multi-UAV system with logarithmic quantizer (42). (a) $Q_l(v_1^u)$ of the first UAV, (b) $Q_l(w_2^u)$ of the second UAV.

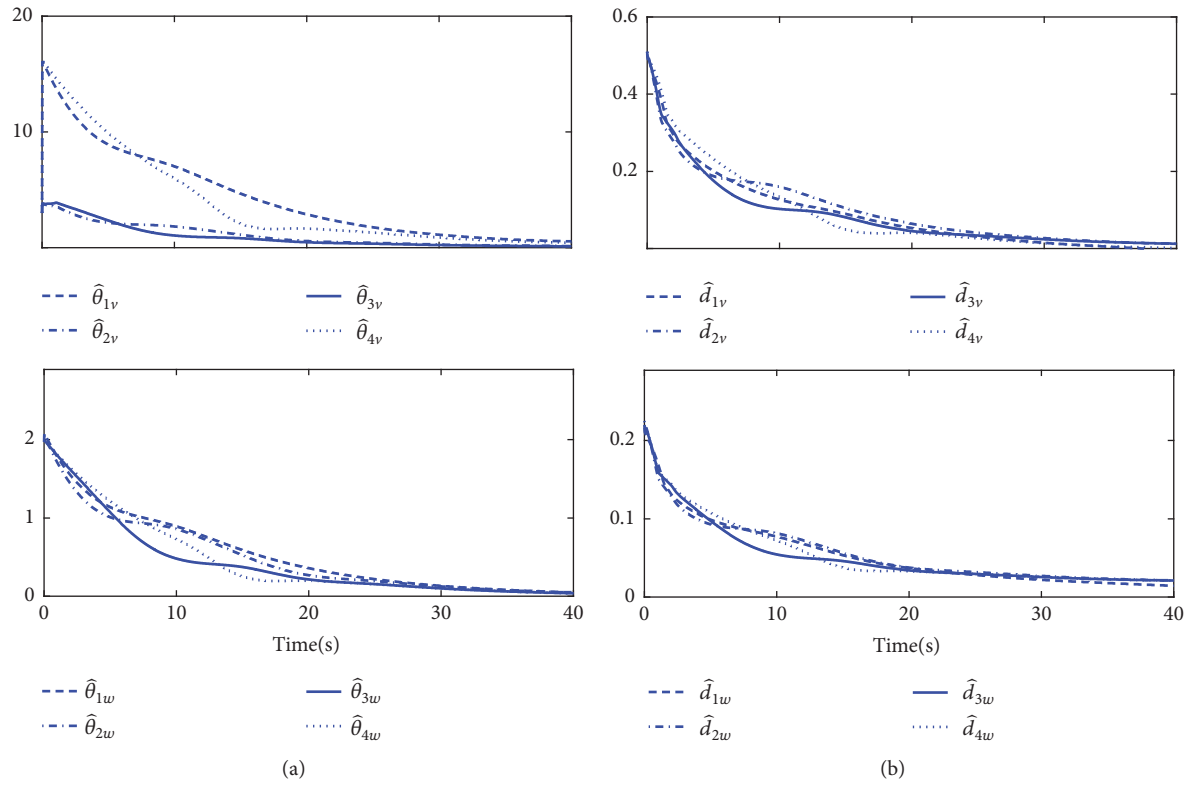

FIGURE 7: Parameter estimations in the multi-UAV system with hysteretic quantizer (3). (a) Estimations of unknown parameters, (b) estimations of unknown disturbances.

these fast switchings are difficult to be transferred via multi-UAV network with a finite data rate channel in practice. In addition, the chattering does great harm to the actuators and UAVs physically. Figures 7 and 8 show the estimations of unknown parameters and disturbances of the multi-UAV systems in the two situations. It can be seen that all the signals in the closed-loop systems are semiglobal finite-time bounded from Figures 3–8. Compared with the multi-UAV system with logarithmic quantizer (42), the multi-UAV system with hysteretic quantizer (3) has better control performance and highly reduces signal chattering.

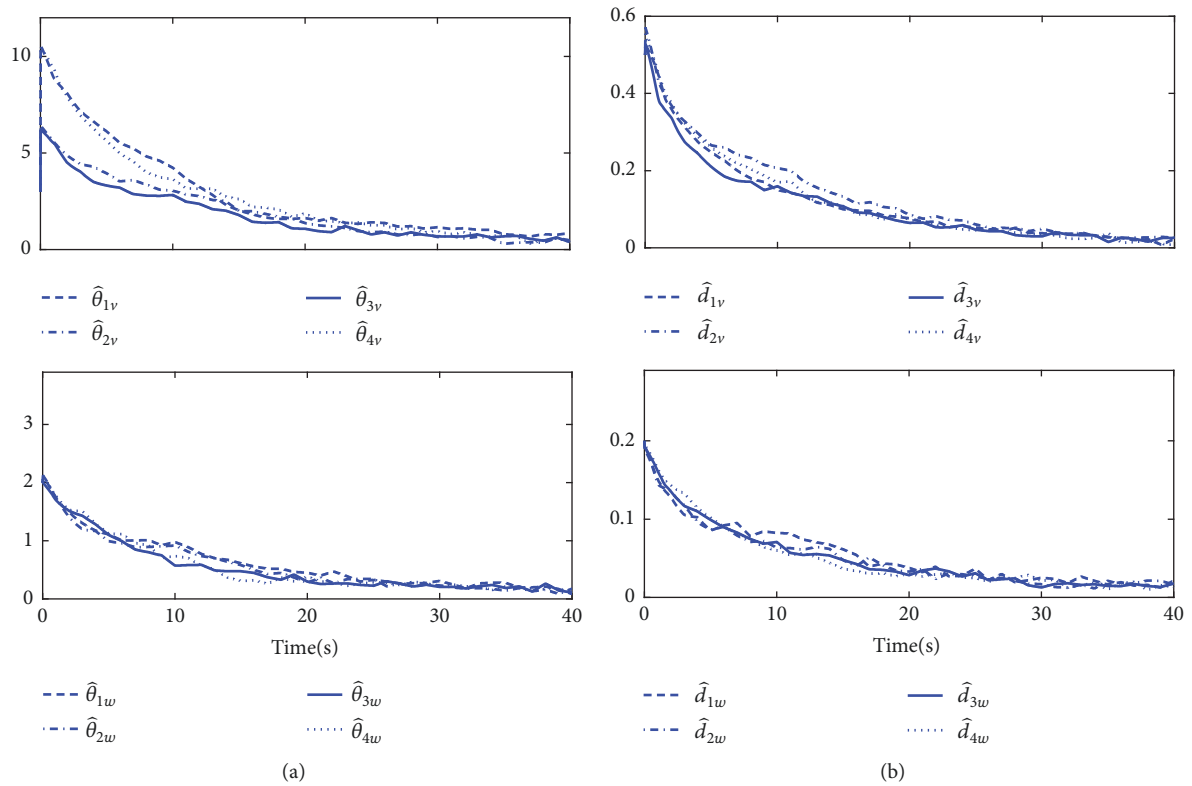

Figure 8: Parameter estimations in the multi-UAV system with logarithmic quantizer (42). (a) Estimations of unknown parameters, (b) estimations of unknown disturbances.

6. Conclusion

Based on the backstepping technique, an adaptive finite-time control scheme is proposed for the time-varying formation tracking of multiple UAVs with inputs quantization. The UAVs are described by kinematic model with nonholonomic constraints and autopilot model with unknown parameters and disturbances. A transverse function method is used to transform the nonholonomic UAV states. To avoid system chattering, the input signals are processed by hysteretic quantizers. A novel decomposition method is utilized to deal with the nonlinearity caused by quantization. The adaptive finite-time controller is established through using the finite-time Lyapunov stability theory and a novel transformation of control signals. With the proposed control design, all the closed-loop signals can keep semiglobal finite-time bounded and the tracking errors can be steered to within a small neighborhood of the origin in finite time. Besides, all the UAVs form and maintain the prescribed formation shape while tracking the reference trajectory. Finally, the simulation results are provided to illustrate the effectiveness of the proposed approach.

Data Availability

The simulation data generated during this study have been deposited with figshare (https://figshare.com/s/76e705aba594fe1969c8). All other data arising from this study are contained within the manuscript.

Conflicts of Interest

The authors declare that there are no conflicts of interest regarding the publication of this paper.

Acknowledgments

The authors gratefully appreciate the partial support of this work by the Aeronautical Science Foundation of China under Grant 20155896025.

References

[1] M. Shi, K. Qin, P. Li, and J. Liu, "Consensus conditions for high-order multiagent systems with nonuniform delays," *Mathematical Problems in Engineering*, Art. ID 7307834, 12 pages, 2017.

[2] J. Huang, "The cooperative output regulation problem of discrete-time linear multi-agent systems by the adaptive distributed observer," *Institute of Electrical and Electronics Engineers Transactions on Automatic Control*, vol. 62, no. 4, pp. 1979–1984, 2017.

[3] L. He, X. Sun, and Y. Lin, "Distributed output-feedback formation tracking control for unmanned aerial vehicles," *International Journal of Systems Science*, vol. 47, no. 16, pp. 3919–3928, 2016.

[4] T. Balch and R. C. Arkin, "Behavior-based formation control for multirobot teams," *IEEE Transactions on Robotics and Automation*, vol. 14, no. 6, pp. 926–939, 1998.

[5] R. W. Beard, J. Lawton, and F. Y. Hadaegh, "A coordination architecture for spacecraft formation control," *IEEE*

Transactions on Control Systems Technology, vol. 9, no. 6, pp. 777–790, 2001.

[6] C. De La Cruz and R. Carelli, "Dynamic model based formation control and obstacle avoidance of multi-robot systems," *Robotica*, vol. 26, no. 3, pp. 345–356, 2008.

[7] D. Liberzon, "Finite data-rate feedback stabilization of switched and hybrid linear systems," *Automatica*, vol. 50, no. 2, pp. 409–420, 2014.

[8] G. Li, Y. Lin, and X. Zhang, "Adaptive output feedback control for a class of nonlinear uncertain systems with quantized input signal," *International Journal of Robust and Nonlinear Control*, vol. 27, no. 1, pp. 169–184, 2017.

[9] D. Liberzon, "Hybrid feedback stabilization of systems with quantized signals," *Automatica*, vol. 39, no. 9, pp. 1543–1554, 2003.

[10] S. Tatikonda and S. Mitter, "Control under communication constraints," *Institute of Electrical and Electronics Engineers Transactions on Automatic Control*, vol. 49, no. 7, pp. 1056–1068, 2004.

[11] J. LaSalle and S. Lefschetz, *Stability by Lyapunov's Direct Method with Application*, Academic Press, New York, NY, USA, 1961.

[12] N. Elia and S. K. Mitter, "Stabilization of linear systems with limited information," *Institute of Electrical and Electronics Engineers Transactions on Automatic Control*, vol. 46, no. 9, pp. 1384–1400, 2001.

[13] B. L. Ma, "Global k-exponential asymptotic stabilization of underactuated surface vessels," *Systems & Control Letters*, vol. 58, pp. 194–201, 2009.

[14] J. Zhou, C. Wen, and G. Yang, "Adaptive backstepping stabilization of nonlinear uncertain systems with quantized input signal," *Institute of Electrical and Electronics Engineers Transactions on Automatic Control*, vol. 59, no. 2, pp. 460–464, 2014.

[15] R. Carli, F. Fagnani, P. Frasca, and S. Zampieri, "Gossip consensus algorithms via quantized communication," *Automatica*, vol. 46, no. 1, pp. 70–80, 2010.

[16] J. J. Fu and J. Z. Wang, "Adaptive coordinated tracking of multi-agent systems with quantized information," *Systems Control Letters*, vol. 74, pp. 115–125, 2014.

[17] Y. Zhu, Y. Zheng, and L. Wang, "Quantised consensus of multi-agent systems with nonlinear dynamics," *International Journal of Systems Science*, vol. 46, no. 11, pp. 2061–2071, 2015.

[18] C.-E. Ren, L. Chen, C. L. P. Chen, and T. Du, "Quantized consensus control for second-order multi-agent systems with nonlinear dynamics," *Neurocomputing*, vol. 175, pp. 529–537, 2015.

[19] B. S. Park, J.-W. Kwon, and H. Kim, "Neural network-based output feedback control for reference tracking of underactuated surface vessels," *Automatica*, vol. 77, pp. 353–359, 2017.

[20] J. Ghommam, M. S. Mahmoud, and M. Saad, "Robust cooperative control for a group of mobile robots with quantized information exchange," *Journal of The Franklin Institute*, vol. 350, no. 8, pp. 2291–2321, 2013.

[21] F. Gao and F. Yuan, "Adaptive finite-time stabilization for a class of uncertain high order nonholonomic systems," *ISA Transactions®*, vol. 54, pp. 75–82, 2015.

[22] X.-N. Shi, Y.-A. Zhang, and D. Zhou, "Almost-Global Finite-Time Trajectory Tracking Control for Quadrotors in the Exponential Coordinates," *IEEE Transactions on Aerospace and Electronic Systems*, vol. 53, no. 1, pp. 91–100, 2017.

[23] S. Yu, X. Yu, B. Shirinzadeh, and Z. Man, "Continuous finite-time control for robotic manipulators with terminal sliding mode," *Automatica*, vol. 41, no. 11, pp. 1957–1964, 2005.

[24] C. Qian and W. Lin, "Non-lipschitz continuous stabilizers for nonlinear systems with uncontrollable unstable linearization," in *Systems Control Letters 42(3*, pp. 185–200, 185-200. doi, 10.1016/S0167-6911(00)00089-X, 2001.

[25] Q. Hu, Y. Yu, B. Li, and J. Qi, "Finite-time attitude tracking control for spacecraft with uncertain actuator configuration," *Proceedings of the Institution of Mechanical Engineers, Part G: Journal of Aerospace Engineering*, vol. 229, no. 13, pp. 2457–2468, 2015.